Methods

Theoretical analysis of a temperature-dependent model of respiratory O₂ consumption using the kinetics of the cytochrome and alternative pathways

Tomomi Inoue[1] iD **and Ko Noguchi[2]** iD

[1]National Institute for Environmental Studies, 16-2 Onogawa Tsukuba, Ibaraki 305-8506, Japan; [2]Department of Life Science, Tokyo University of Pharmacy and Life Sciences, 1432-1

Horinouchi Hachioji, Tokyo 192-0392, Japan

Author for correspondence:
Tomomi Inoue
Email: tomomi.inoue@nies.go.jp

Received: *16 July 2020*
Accepted: *14 September 2020*

Summary

- Temperature dependence of plant respiratory O₂-consumption has been empirically described by the Arrhenius equation. The slope of the Arrhenius plot (which is proportional to activation energy) sometimes deviates from a constant value. We conducted kinetic model simulations of mitochondrial electron flow dynamics to clarify factors affecting the shape of the Arrhenius plot.
- We constructed a kinetic model of respiration in which competitive O₂-consumption by the cytochrome pathway (CP) and the alternative pathway (AP) were considered, and we used this model to describe the temperature dependence of respiratory O₂-consumption of Arabidopsis.
- The model indicated that the electron partitioning and activation energy differences between CP and AP were reflected in the slope and magnitude of the dependent variables of the Arrhenius plot. When the electron partitioning and activation energies of CP and AP were constant with temperature change, our model suggested that the Arrhenius plot would be almost linear. When the electron partitioning or activation energy of CP, or both, rapidly changed with temperature, the Arrhenius plot deviated from linearity, as reported in previous experimental studies.
- Our simulation analysis quantitatively linked the kinetic model parameters with physiological mechanisms underlying the instantaneous temperature dependence of plant respiration rate.

Introduction

In the respiratory chain of plant mitochondria, complex IV (cytochrome *c* oxidase; COX) and the alternative oxidase (AOX) pass electrons to oxygen (O₂) (Fig. 1). The cytochrome pathway (CP) includes complex III, cytochrome *c* and COX; the alternative pathway (AP) includes AOX. These two pathways share a common component – the branching point between them, identified as ubiquinone (UQ) (Del-Saz *et al.*, 2018). Reported observations support the 'electron competition model' that CP and AP competitively consume electrons (Ribas-Carbo *et al.*, 1995; Del-Saz *et al.*, 2018). Bypassing CP by partitioning electrons to AP does not contribute to the proton electrochemical gradient, and it decreases respiratory ATP production by approximately two-thirds. Although AP seems to be energetically wasteful, it contributes to the thermogenic metabolism of some highly specialized flowers (Seymour, 2001), and in many nonthermogenic plants, rapid upregulation of AOX decreases the concentrations of reactive oxygen species under various environmental stresses

(Vanlerberghe & McIntosh, 1997; Moore *et al.*, 2002; Millenaar & Lambers, 2003). Alternative oxidase most likely represents an adaptive feature of sessile plants. The responses of these two O₂-consuming pathways have intrigued many researchers studying the physiological responses of plants to their living environments.

The O₂-consumption rate is a convenient index for assessing electron flow in the respiratory system. The rate of consumption of O₂ by the mitochondrial respiratory chain can be explained by a chemical reaction in which O₂ is reduced to water. The rate of a chemical reaction is controlled by the energy barrier (i.e. activation energy E) between the reactants (O₂) and the products (H₂O). The activation energy can be calculated from the instantaneous temperature dependence of the reaction rate, which is the slope of the Arrhenius plot given by the following equation:

$$k = Ae^{-\frac{E}{RT}} \qquad \text{Eqn 1}$$

where k is the rate constant of the reaction (s⁻¹), A is the pre-exponential factor (s⁻¹), which is often called frequency factor, E is
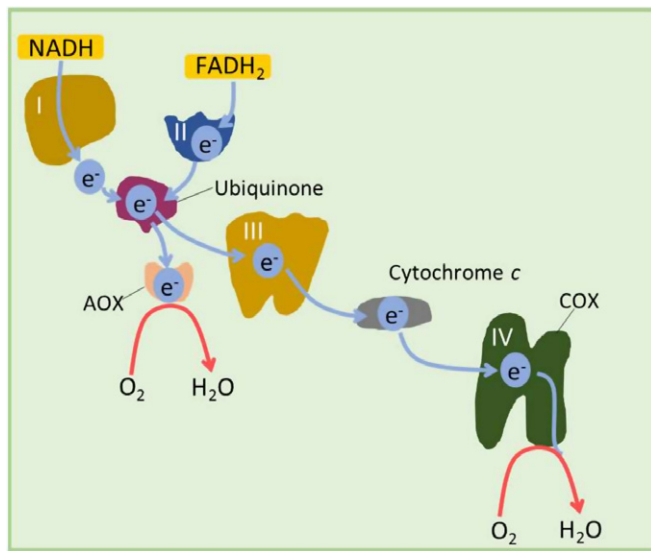
Fig. 1 Electron flow in the respiratory chain. Blue arrows indicate electron flow, and red arrows indicate oxygen reduction to water in AP and CP. AOX, alternative oxidase; COX, cytochrome c oxidase; e$^-$, electron; FADH$_2$, flavin adenine dinucleotide; NADH, nicotinamide adenine dinucleotide.

the activation energy (J mol^{-1}), R is the gas constant (8.314 J mol^{-1} K^{-1}) and T is absolute temperature (K). In previous studies, the following Q_{10}-model has often been used for the instantaneous temperature dependence of plant respiration rates (Tjoelker et al., 2001; Atkin & Tjoelker, 2003):

$$Q_{10} = \left(\frac{r}{r_{REF}}\right)^{\left[\frac{10}{T-T_{REF}}\right]} \qquad \text{Eqn 2}$$

where r is the rate of respiration at a certain temperature T and r_{REF} is the rate at a temperature 10°C lower than T (T_{REF}). Lloyd & Taylor (1994) have suggested a modified Arrhenius equation for plant respiration (Eqn 3), in which the instantaneous temperature dependence of the plant respiration rate is quantified by a parameter E, which is assumed to be constant.

$$r = r_{REF} \times e^{\frac{E}{R} \times \left[\frac{1}{T_{REF}} - \frac{1}{T}\right]} = r_{REF} \times e^{\frac{E}{R} \times \left[\frac{T-T_{REF}}{T \times T_{REF}}\right]} \qquad \text{Eqn 3}$$

However, in some cases, Arrhenius plots of experimentally measured respiratory O$_2$-consumption and CO$_2$ efflux rates deviate from linearity. This deviation indicates that the E for plant respiration is not necessarily constant and could be temperature dependent. Kruse & Adams (2008) have used a second-order polynomial approximation to describe the instantaneous temperature dependence of E:

$$\log_e(r) = \log_e(r_{REF}) + \frac{E(T_{REF})}{R} \times \frac{T - T_{REF}}{T \times T_{REF}}$$
$$+ \delta(T_{REF}) \times \left[\frac{T - T_{REF}}{T \times T_{REF}}\right]^2 \qquad \text{Eqn 4}$$

where $E(T_{REF})$ is the temperature dependence of the plant respiration rate at the reference temperature and $\delta(T_{REF})$ is a

factor that accounts for the dynamic response of E to temperature. The integrated value of the right side of Eqn 4 over a distinct temperature interval is called *Cap(r)* and is considered to be a measure of respiratory capacity (Kruse et al., 2011). This model fits the experimental data in nonlinear Arrhenius plots well (Kruse et al., 2018), and calculating the values of E (T_{REF}), $\delta(T_{REF})$ and *Cap(r)* enables the exploration of respiratory properties (Noguchi et al., 2015). Heskel et al. (2016) have analysed a large number of measurements of leaf CO$_2$ efflux rates for 231 species from 7 biomes by using a second-order log-polynomial (LP) model, and they have estimated the coefficients needed to predict leaf CO$_2$ respiration–temperature relationships. In the LP model, the quadratic coefficient, c, represents the temperature dependence of the slope of the $\log_e(r)$ vs T relationship (O'Sullivan et al., 2013). However, few details are known about the mechanism that determines the instantaneous temperature dependence of E or how the factors $\delta(T_{REF})$ in the modified Arrhenius model and c in the LP model should be interpreted.

Hobbs et al. (2013) have advocated macromolecular rate theory (MMRT) to explain the instantaneous temperature dependence of Arrhenius plots in enzyme-catalysed biochemical reactions. The theory is that the heat capacity (C_p) for the enzyme–transition state complex is generally lower than that of the enzyme–substrate complex, which is not as rigid, and the difference in those heat capacities, $\Delta C_p^{\ddagger}$, is not negligible in biochemical reactions because of the high molecular weight of enzymes. On the basis of MMRT, the natural logarithm of the rate constant of the reaction (k) is given by the following equation:

$$\log_e k = \log_e \frac{k_B T}{h} - \left[\frac{\Delta H_{T_0}^{\ddagger} + \Delta C_p^{\ddagger}(T - T_{REF})}{RT}\right]$$
$$+ \left[\frac{\Delta S_{T_0}^{\ddagger} + \Delta C_p^{\ddagger}(\log_e T - \log_e T_{REF})}{R}\right], \qquad \text{Eqn 5}$$

where k_B and h are Boltzmann's and Planck's constants, respectively, and $\Delta H_{T_0}^{\ddagger}$ and $\Delta S_{T_0}^{\ddagger}$ are the differences in enthalpy and entropy between the ground state and the transition state, respectively, at reference temperature T_{REF}.

This model clearly accounts for the fact that the slope of the Arrhenius plot of enzyme-catalysed biochemical reactions can deviate from linearity (Schipper et al., 2014; Arcus et al., 2016). Also, MMRT can explain the short-term temperature dependence of leaf CO$_2$ efflux rates as well as the LP model (Liang et al., 2018). The MMRT can therefore be applied to respiratory O$_2$-consumption in plants.

In plant respiratory systems, respiratory CO$_2$ is produced mainly by the pyruvate dehydrogenase complex and the TCA cycle, and its efflux is regulated by various cellular processes. By contrast, plant O$_2$-consumption is mediated by two pathways, CP and AP, and the temperature dependence of the O$_2$-consumption rate should therefore be determined by the kinetics of CP and AP. Kruse et al. (2011) have surveyed reports on the

instantaneous temperature dependence of plant O_2-consumption rates and have concluded that, in most cases, E depends on which pathway – CP or AP – dominates the electron flux. The electron partitioning between CP and AP is regulated by the collision frequency at each enzyme and the activation energy for each pathway. A change in electron partitioning is therefore a possible explanation for the deviation from linearity of some Arrhenius plots of plant O_2-consumption rates. Kerbler *et al.* (2019) have found that the instantaneous temperature dependence of ATP synthase hydrolysis differs from that of NADH oxidation in isolated mitochondria of Arabidopsis. This result suggests that the rate-determining step within the CP, which consists of multiple components, can vary, and a change of the rate-determining step with temperature change may cause a change in the E of the CP and lead to nonlinearity of the Arrhenius plot of O_2-consumption rates. However, it is still unclear how two factors – the temperature dependence of the E of CP and electron partitioning between CP and AP – quantitatively affect the nonlinearity of the Arrhenius plot of O_2-consumption rates.

In this study, we constructed a kinetic model of plant O_2-consumption rates that took into consideration competitive O_2-consumption by CP and AP. We used the kinetic model to describe the instantaneous temperature dependence of respiratory O_2-consumption. We conducted several simulations to identify how competitive O_2-consumption could affect the shape of the Arrhenius plot of O_2-consumption rate. Next, we fitted the kinetic model to the experimental leaf O_2-consumption-rate data, and we examined what parameters in the kinetic model were most responsible for the nonlinearity of the Arrhenius plot of O_2-consumption rates. Finally, we discuss the physiological mechanisms underlying the instantaneous temperature dependence of respiratory O_2-consumption on the basis of the kinetic model.

Materials and Methods

Temperature dependence of the rate of oxygen consumption by plant mitochondria

O_2 reduction by an enzyme can be expressed by the following equation, based on Michaelis–Menten kinetics:

$$[E] + [O_2] \underset{k_{-1}}{\overset{k_1}{\rightleftarrows}} [EO_2] \xrightarrow{k_2} [E] + 2[H_2O] \quad \overset{4H^+}{} \tag{Eqn 6}$$
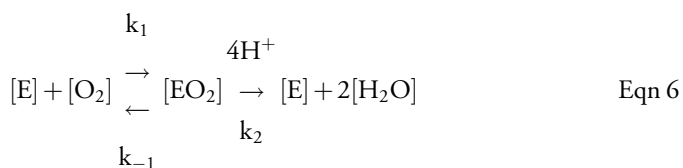
where $[E]$ is the concentration of the active enzyme, $[EO_2]$ is the concentration of the O_2–enzyme complex in the transition state, and the k parameters are the rate constants corresponding to the reactions indicated by the arrows.

When electrons are continuously supplied in plant cells from the upstream citric acid cycle and the CP and AP simultaneously share electrons, the $[O_2]$ dynamics in the measurement system

can be expressed as follows. (Supporting Information Notes S1 contains a detailed description.)

$$-\frac{d[O_2]}{dt} = k_{2aox}[EO_2]_{aox} + k_{2cox}[EO_2]_{cox}$$

$$= \left(\alpha \frac{k_{2aox}k_{1aox}[O_2]}{k_{-1aox} + k_{2aox} + k_{1aox}[O_2]} + \frac{k_{2cox}k_{1cox}[O_2]}{k_{-1cox} + k_{2cox} + k_{1cox}[O_2]} \right)[E]_{0cox}$$

$$= K[E]_{0cox} \tag{Eqn 7}$$

where $[E]_{0cox}$ is the concentration of the active components of CP (complex III, cytochrome c and COX) in the measurement system, $[E]_{0aox}$ is the concentration of active AOX, and α is the ratio of $[E]_{0aox}$ to $[E]_{0cox}$. The parameter K is the observed rate constant for the rate of O_2-consumption in the measurement system and is defined in Eqn 8. The Michaelis constants for CP ($k_{m\ cox}$) and AP ($k_{m\ aox}$) are defined by Eqns 9 and 10, respectively.

$$K = \frac{\alpha k_{2aox}[O_2]}{k_{m\ aox} + [O_2]} + \frac{k_{2cox}[O_2]}{k_{m\ cox} + [O_2]}$$
$$= \left(\frac{\alpha k_{2aox}[O_2]}{k_{m\ aox} + [O_2]} \right) \left\{ 1 + \frac{1}{\alpha} \left(\frac{k_{2cox}}{k_{2aox}} \right) \left(\frac{k_{m\ aox} + [O_2]}{k_{m\ cox} + [O_2]} \right) \right\}, \tag{Eqn 8}$$

$$k_{m\ cox} = \frac{k_{2cox} + k_{-1cox}}{k_{1cox}}, \tag{Eqn 9}$$

$$k_{m\ aox} = \frac{k_{2aox} + k_{-1aox}}{k_{1aox}} \tag{Eqn 10}$$

The relationship between K^{-1} and $[O_2]^{-1}$ is expressed as follows:

$$K^{-1} = \left[\left(\frac{\alpha k_{2aox}[O_2]}{k_{m\ aox} + [O_2]} \right) \left\{ 1 + \frac{1}{\alpha} \left(\frac{k_{2cox}}{k_{2aox}} \right) \left(\frac{k_{m\ aox} + [O_2]}{k_{m\ cox} + [O_2]} \right) \right\} \right]^{-1}$$

$$= \frac{1}{\alpha} \left(\frac{k_{m\ aox}}{k_{2aox}[O_2]} + \frac{1}{k_{2aox}} \right) \left\{ \frac{\alpha k_{2aox}(k_{m\ cox} + [O_2])}{\alpha k_{2aox}(k_{m\ cox} + [O_2]) + k_{2cox}(k_{m\ aox} + [O_2])} \right\}$$

$$= \frac{1}{\alpha} \left(\frac{k_{m\ aox}}{k_{2aox}[O_2]} + \frac{1}{k_{2aox}} \right) \left\{ \frac{\alpha k_{2aox} \left(\frac{k_{m\ cox}}{[O_2]} + 1 \right)}{\alpha k_{2aox} \left(\frac{k_{m\ cox}}{[O_2]} + 1 \right) + k_{2cox} \left(\frac{k_{m\ aox}}{[O_2]} + 1 \right)} \right\}, \tag{Eqn 11}$$

We can therefore calculate $(\alpha k_{2aox} + k_{2cox})$ from the reciprocal of the y-intercept of the plot of K^{-1} vs $[O_2]^{-1}$ – that is, by substituting zero for $[O_2]^{-1}$ in Eqn 11, or by measuring K when $[O_2]$ is much greater than $k_{m\ cox}$ and $k_{m\ aox}$ (i.e. the reaction rate is a maximum). More details are provided in Notes S1.

On the basis of the Arrhenius equation (Eqn 1), the instantaneous temperature dependence of $(\alpha k_{2aox} + k_{2cox})$, which can be measured experimentally, is expressed as follows:

$$\log_e(\alpha k_{2aox} + k_{2cox})$$

$$= \log_e\left\{\alpha A_{aox}\exp\left(\frac{-E_{aox}}{RT}\right) + A_{cox}\exp\left(\frac{-E_{cox}}{RT}\right)\right\}$$

$$= \log_e\left[\left\{A_{cox}\exp\left(\frac{-E_{cox}}{RT}\right)\right\}\left\{1 + \alpha\frac{A_{aox}}{A_{cox}}\exp\left(\frac{\Delta E}{RT}\right)\right\}\right]$$

$$= \log_e A_{cox} - \frac{E_{cox}}{RT} + \varepsilon$$

$$\text{Eqn 12}$$

where A_{cox} and A_{aox} are pre-exponential factors related to CP and AP, respectively, ΔE is the difference between the activation energies associated with O_2 reduction by CP (E_{cox}) and AP (E_{aox}), and ε is the AP-contribution term expressed by Eqn 13.

$$\varepsilon = \log_e\left\{1 + \alpha\frac{A_{aox}}{A_{cox}}\exp\left(\frac{\Delta E}{RT}\right)\right\} \qquad \text{Eqn 13}$$

The apparent y-intercept of the plot of $\log_e(\alpha k_{2aox} + k_{2cox})$ vs T^{-1}, $\log_e A_{overall}$, can be obtained from Eqn 14 (derived by substituting zero for T^{-1} in Eqn 12):

$$\log_e A_{overall} = \log_e(A_{cox} + \alpha A_{aox}), \qquad \text{Eqn 14}$$

The apparent slope (i.e apparent activation energy) can be obtained by differentiation of the right side of Eqn 12 with respect to T^{-1}, as follows. (Details are provided in Notes S1).

$$\frac{d\log_e(\alpha k_{2aox} + k_{2cox})}{dT^{-1}} = \frac{-E_{cox}}{R} + \frac{\Delta E}{R}\left\{\frac{1}{\frac{A_{cox}}{\alpha A_{aox}}\exp\left(\frac{-\Delta E}{RT}\right) + 1}\right\}$$

$$= \frac{-E_{cox} + \gamma}{R},$$

$$\text{Eqn 15}$$

where γ is the AP-contribution term expressed by Eqn 16.

$$\gamma = \Delta E\left\{\frac{A_{cox}}{\alpha A_{aox}}\exp\left(\frac{-\Delta E}{RT}\right) + 1\right\}^{-1}, \qquad \text{Eqn 16}$$

In this study, the value of α reflected the relative amounts of active enzymes of CP and AP. Two other metrics, ε and γ, reflected the additional effects of the AP on the O_2-consumption rate and the slope of the Arrhenius plot (i.e. activation energy).

Simulations

With these models, we examined whether two factors, α, the ratio $[E]_{0aox} : [E]_{0cox}$, and ΔE, the difference between E_{cox} and E_{aox}, affected the nonlinearity of the Arrhenius plot. We then simulated the instantaneous temperature dependence of plant O_2-consumption rates under various combinations of α and ΔE in the temperature range 10–40°C. In accordance with the results of previous studies (Kruse *et al.*, 2011), we set E_{aox} to be lower than E_{cox} ($\Delta E > 0$). We first examined the effects of α

and ΔE, not only on O_2-consumption rates but also on the AP-contribution terms, ε and γ. We performed the first three of the following simulations by using various combinations of ΔE (5, 10, 20 and 40 kJ mol^{-1}) and α (0.1, 0.3 and 0.5) and assuming ΔE and α to be independent of temperature. In simulations (4) and (5), α and ΔE, respectively, were functions of temperature.

(**1**) Instantaneous temperature dependence of plant O_2-consumption rate (Eqn 12)
(**2**) Instantaneous temperature dependence of the AP-contribution term ε (Eqn 13)
(**3**) Instantaneous temperature dependence of the AP-contribution term γ (Eqn 16)
(**4**) Instantaneous temperature dependence of plant O_2-consumption rate on the assumption that α gradually changed from 0.0 to 0.5 in response to temperature changes.
(**5**) Instantaneous temperature dependence of plant O_2-consumption rate on the assumption that the activation energy of CP, E_{cox}, gradually changed from 25 to 30 kJ mol^{-1} in response to temperature changes.

In simulations (1) and (3), A_{aox}/A_{cox} was equated to α under the assumption that the collision frequency (quantified by the pre-exponential factor A) corresponded to the concentration of active enzyme, either $[E]_{0cox}$ or $[E]_{0aox}$. In simulation (1), the intercept $\log_e A_{overall}$ was set to 28, and the activation energy of AP (E_{aox}) was set as 20 kJ mol^{-1}.

Next, we validated the effect on the curvature of the Arrhenius plot of an abrupt change of α or ΔE due to a change in temperature. When ΔE changed with the measurement temperature, we assumed that the temperature dependence of CP could vary for the following two reasons. First, CP consists of multiple components, including complex III, cytochrome c and COX; we therefore assumed that the activation energy would vary as a function of the status of each component. In addition, the CP components interact with each other and form an active super-complex that functions as an oxidative phosphorylation system (Dudkina *et al.*, 2010; Milenkovic *et al.*, 2017). The activation energy of CP could thus vary because of the large heat capacity of the components in the context of MMRT. By contrast, we fixed the activation energy of AP because electron transport through AP is performed by a single small enzyme, AOX. Changes are therefore less likely in E_{aox} than in E_{cox}. However, if the AOX structure is drastically changed by its activation state or the surrounding conditions, or both, E_{aox} may be changed. In this study, we fixed E_{aox} to simplify the simulations. We performed the following two simulations on the assumption that either α or ΔE could change in response to instantaneous temperature changes. In simulations (4) and (5), the intercept $\log_e A_{overall}$ was set to 28, and the activation energy of AP (E_{aox}) was set as 20 kJ mol^{-1}. In simulation (4), ΔE was set as 10 kJ mol^{-1}.

The simulations were performed using R v.3.6.2 (R Core Team, 2019).

Measurement of leaf O_2-consumption rate and fitting the kinetic model to experimental data

Experimental O_2-consumption rates were measured with leaves of *Arabidopsis thaliana* (Fei-0) for the Arrhenius plot. Arabidopsis

seeds were sown in plastic pots filled with a water-saturated, 1 : 1 mixture of soil (Pro-Mix HP, Premier Tech Horticulture, Pointe-Lebel, Quebec, Canada) and vermiculite (Fukushima Vermi Ltd, Fukushima, Japan). After being incubated at 4°C in the dark for 5 d, plants were grown for 2 wk at 15°C or 25°C, 60% relative humidity, and 100 μmol quanta m^{-2} s^{-1} of visible light for 10 h d^{-1} in growth chambers. From that time onward, the plants were fertilised twice a day until the end of the study with a Hyponex nutrient solution (N : P : K = 6 : 10 : 5) (HYPONeX Japan, Osaka, Japan) diluted 1 : 2000 with water. After 2 wk of cultivation, individual leaf O$_2$ respiration rates were measured for five randomly selected seedlings at each growth temperature. For each seedling, leaves were detached into a 50-ml glass vial, and the O$_2$-consumption rate was measured with a fluorescence O$_2$ sensor (FDO925; Xylem Analytics, Freis-taat Bayern, Germany) in the dark at 15, 20, 25, 30 and 35°C. After the O$_2$-consumption rate had been recorded at each temperature, the sample in the vial was retrieved and dried at 80°C until the weight was constant. The final weight was recorded. The O$_2$-consumption rate was expressed on this dry-weight basis.

The modified Arrhenius model (Eqn 4) was fitted to the experimental data to obtain the curvatures of the Arrhenius plots, and then the kinetic model (Eqn 12) was fitted to the curves to examine the effects of α and E_{cox} on the shape of the Arrhenius plots. Although Eqn 12 has five variables, three variables (E_{aox}, A_{aox}, and A_{cox}) were assumed to be constant, and thus the model included two independent variables, α and ΔE. The fitting exercises were performed by letting α vary in the range 0.1–2.0 as a function of the measurement temperature on the assumption that E_{aox} and E_{cox} were independent of temperature, and letting E_{cox} vary as a function of the measurement temperature on the assumption that α and E_{aox} were both independent of temperature. E_{aox} was set to 15 kJ mol^{-1} or 20 kJ mol^{-1}, and E_{cox} was chosen subject to the constraint that $E_{cox} > E_{aox}$. The intercept, $\log_e A_{overalb}$ was set to 18 because the Arrhenius plot obtained when only CP was engaged (i.e. $\alpha = 0$) was lower than the observed curves. The simulations were performed using R v.3.6.2 (R Core Team, 2019).

Results

Simulation results when α and ΔE were constant, independent of measurement temperature

The instantaneous temperature dependence of plant O$_2$-consumption rates are potentially influenced by both CP and AP. According to Eqn 12, the temperature dependence of the O$_2$-consumption rate can be obtained by adding the AP-contribution term ε (Eqn 13) to the Arrhenius equation obtained when only CP is engaged (i.e. $\alpha = 0$).

The AP-contribution term ε is always positive (i.e. the logarithm of $\left\{1 + \frac{[E]_{0\ aox} A_{aox}}{[E]_{0\ cox} A_{cox}} \exp\left(\frac{\Delta E}{RT}\right)\right\} > 1$). Thus, as long as electrons flowed to AP, the Arrhenius plot of plant O$_2$-consumption rate was always above the plot obtained when only CP was engaged (i.e, $\alpha = 0$; black solid line, Fig. 2a–d). Here, we assumed that $E_{aox} < E_{cox}$ on the basis of previous reports that the activation energy of CP is often, but not always, larger than that of AP

(Kruse *et al.*, 2011). If, instead, the activation energy of AP was larger than that of CP ($E_{aox} > E_{cox}$), then as long as electrons flowed to AP, the Arrhenius plot would be lower than the plot when only CP was present (not shown here).

On the assumption that α and ΔE were constant while the temperatures were being varied, the AP-contribution term ε was negatively correlated with temperature (i.e. positively correlated with T^{-1} in Eqn 13, Fig. 2e–h). Furthermore, ε became more sensitive to temperature as ΔE increased (Fig. 2e–h). Fig. 3 shows the slope deviation, γ, for several combinations of α and ΔE. According to Eqn 16, γ is defined as the product of ΔE and the temperature-dependent term $\left\{\frac{A_{cox}}{\alpha A_{aox}} \exp\left(\frac{-\Delta E}{RT}\right) + 1\right\}^{-1}$. Because the temperature-dependent term ranges from 0 to 1, γ always falls between 0 and ΔE. The value of γ approaches ΔE as the relative weight ratio of the active AOX enzyme and electron flow to AP increase – that is, as A_{aox} and α increase (Eqn 16). If $E_{aox} < E_{cox}$, the fact that $\gamma > 0$ indicates that electron flow to AP has the effect of decreasing the slope of the Arrhenius plot (Eqn 15). Because γ depends on temperature, γ can cause the apparent overall activation energy to depend on the instantaneous temperature. However, the effects of temperature on γ in the simulations, which were based on realistic situations, were extremely small (Fig. 3), and Arrhenius plots of O$_2$-consumption rate vs temperature were almost linear (Fig. 2a–d). As shown in Eqn 14, the apparent y-intercept of the Arrhenius plot, which can be interpreted as a collision frequency, can be expressed in terms of α and the pre-exponential factors A for both CP and AP. The implication is that the apparent y-intercept can be used as a metric of the contents of the CP and AOX or O$_2$ accessibility to these terminal enzymes, or both.

Simulation results when α or ΔE varies in response to measurement temperature

Simulations (1)–(3), described in 'Simulations' in the Materials and Methods section, above, suggested that the Arrhenius plot is almost linear when E and α are independent of temperature, and thus the effect of a rapid change of E_{cox} or α caused by a temperature change on the curvature of the Arrhenius plot was validated here. In simulation (4), when α changed (0.1–0.5) monotonically with increasing temperature (10–40°C), the simulated Arrhenius plots deviated from linearity (Fig. 4, Fig. S1). The shapes of the plots resembled the shapes of the corresponding plots of the instantaneous temperature dependence of α (compare Fig. 4a and e, b and f, c and g, and d and h). The shape of the Arrhenius plot was convex (Fig. 4) or concave (Fig. S1), depending on the behaviour of α. In some cases, the slope of the Arrhenius plot was positive when α decreased with increasing temperature (Fig. 4f, g, Fig. S1f, g).

In simulation (5), ΔE changed (5–10 kJ mol^{-1}) monotonically with increasing temperature (10–40°C), and the slope of the Arrhenius plot increased in accordance with the low α (Fig. 5). The shape of the Arrhenius plot was convex when the shape of ΔE changes became concave, and it was concave when the shape of the ΔE changes became convex. Furthermore, in some cases, the sign of the slope of the Arrhenius plot was positive
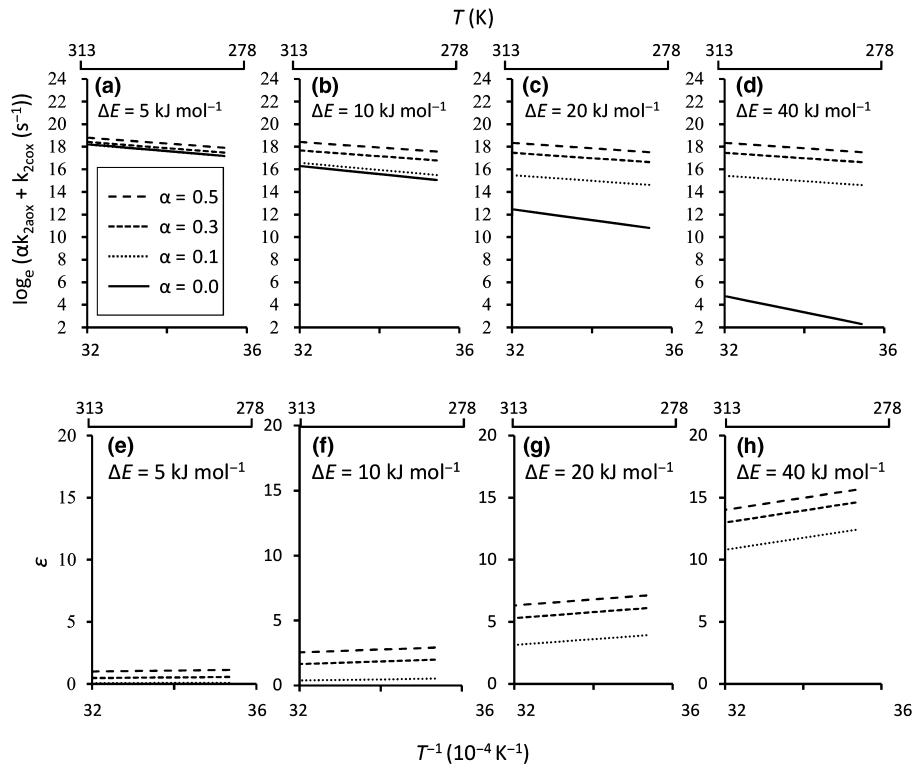
Fig. 2 Simulated Arrhenius plots, based on the assumption that ΔE and α are constant across the temperature range (a–d), and there is instantaneous temperature dependence of the AP-contribution term ε (e–h). The simulation was conducted with various combinations of ΔE (5, 10, 20 and 40 kJ mol^{-1}) and α (0.1, 0.3 and 0.5). E_{aox} was set to 20 kJ mol^{-1}. In (a–d), the black line indicates the Arrhenius plot when $\alpha = 0$ (no electron flow to AP). The temperature dependence of ε is zero when $\alpha = 0$. A_{cox}, pre-exponential factors related to CP; α, the ratio $[E]_{0aox} : [E]_{0cox}$; $[E]_{0aox}$, the concentration of active AOX in the measurement system; $[E]_{0cox}$, the concentration of active CP in the measurement system; ΔE, the difference in activation energy between O_2 reduction by CP (E_{cox}) and by AP (E_{aox}); ε, the AP-contribution term in Eqn 13.

when ΔE increased with increasing temperature. In those cases, the activation energy of the CP increased with temperature. The activation energy of AP was assumed to be constant at 20 kJ mol^{-1} for all cases in this simulation.

Fitting the kinetic model to experimental data

According to simulations (1)–(5), a curved Arrhenius plot was satisfactorily explained by allowing α or E_{cox} to vary with the measurement temperature. Fitting the kinetic model to experimental leaf O_2-consumption rates identified possible values of α and E_{cox}, as well as the contribution of the temperature dependence of each parameter on the slope of Arrhenius plot.

Leaf O_2-consumption rates were higher for plants grown at 15°C than at 25°C throughout the range of measurement temperatures (Fig. 6a). The Arrhenius plot obtained deviated from linearity in both growth–temperature treatments, and the shape of the curve was convex for the plants grown at 25°C (i.e. there was less temperature dependence as the temperature increased) and concave for the plants grown at 15°C (i.e. there was more temperature dependence as the temperature increased) (Fig. 6a).

The kinetic model given by Eqn 12 was fitted to the obtained curve at each growth temperature. In the fitting procedure, we changed α or E_{cox} with measurement temperature, subject to the constraint that the other parameter was constant. The kinetic model described the curvature of the observed Arrhenius plots well (solid lines in Fig. 6a).

When E_{cox} and E_{aox} were independent of measurement temperature, the value of α corresponding to the observed Arrhenius curvature was plotted against the measurement temperature (Fig. 6b). The calculations were done by using two values of E_{aox}, namely 15 and 20 kJ mol^{-1}. For both E_{aox} values, α was higher in the plants grown at 15°C than at 25°C throughout the range of measurement temperatures (Fig. 6b). The value of α increased as the leaf O_2-consumption rate increased at higher measurement temperatures, and the shapes of the α-curves were similar to the observed Arrhenius plots: convex in plants grown at 25°C and concave in plants grown at 15°C. Fig. 6b shows the behaviour of the temperature dependence of α when E_{cox} was increased from 21 kJ mol^{-1} in increments of 2 kJ mol^{-1}. The value of α increased as the E_{cox} increased, and the α-curves tended to converge. Whereas the shape of the convergent α curves depended on the value of E_{aox}, α was higher in plants grown at 15°C than at 25°C throughout the range of measurement temperatures. As a result, the kinetic model that incorporated the 'temperature dependence of α' explained the experimental data well.

Next, the E_{cox} corresponding to the observed Arrhenius curvature was plotted against the measurement temperature subject to the condition that α was independent of temperature (Fig. 6c).
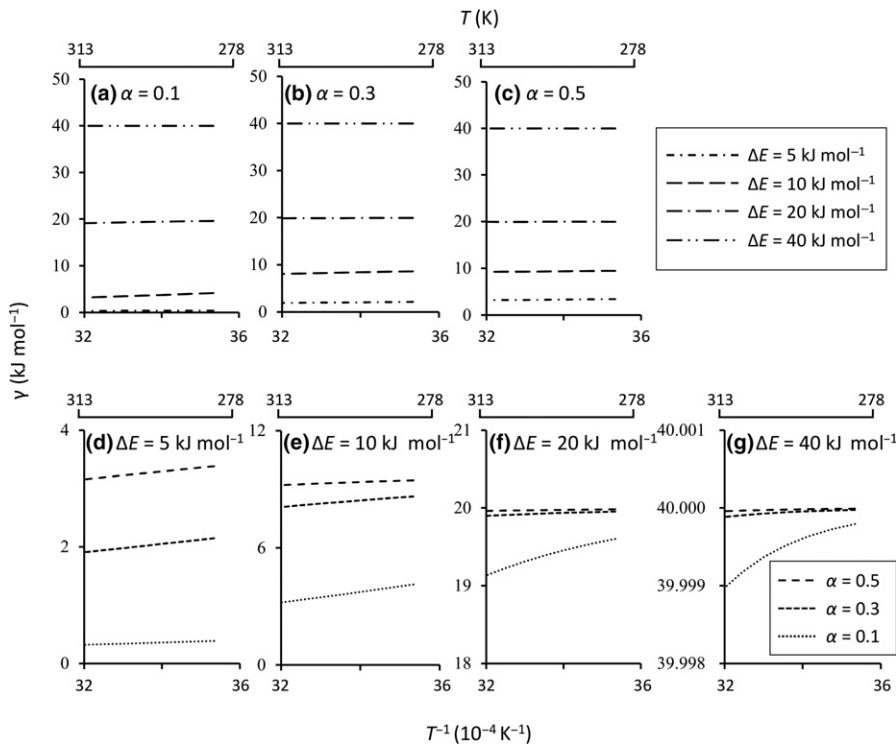
Fig. 3 Instantaneous temperature dependence of the AP-contribution term γ under various combinations of α (0.1, 0.3 and 0.5) (a–c) and ΔE (5, 10, 20 and 40 kJ mol^{-1}) (d–g). E_{aox} was set to 20 kJ mol^{-1}. α, the ratio [E]$_{0aox}$: [E]$_{0cox}$; [E]$_{0aox}$, the concentration of active AOX in the measurement system; [E]$_{0cox}$, the concentration of active CP in the measurement system; ΔE, the difference in the activation energy between O$_2$ reduction by CP (E_{cox}) and by AP (E_{aox}); γ, the AP-contribution term in Eqn 16.

As in Fig. 6b, we performed the calculations at two values of E_{aox}, namely 15 and 20 kJ mol^{-1}. The candidate values of α satisfying the observed Arrhenius curvature were bounded. The possible range of α depended on the combination of E_{aox} and growth temperature: $0.1 < \alpha < 0.3$ when $E_{aox} = 15$ kJ mol^{-1} for plants grown at 15°C; $\alpha = 1.3$ when $E_{aox} = 20$ kJ mol^{-1} for plants grown at 15°C; $0.1 < \alpha < 0.2$ when $E_{aox} = 15$ kJ mol^{-1} for plants grown at 25°C; and $0.2 < \alpha < 0.7$ when $E_{aox} = 20$ kJ mol^{-1} for plants grown at 25°C (Fig. 6c). The range of E_{cox} values was higher for plants grown at 25°C (21.5–29.0 kJ mol^{-1} when E_{aox} equalled 15 kJ mol^{-1} and 21.2–32.0 kJ mol^{-1} when E_{aox} equalled 20 kJ mol^{-1}) than for plants grown at 15°C (19.7–22.5 kJ mol^{-1} when E_{aox} equalled 15 kJ mol^{-1} and 20.2–24.0 kJ mol^{-1} when E_{aox} equalled 20 kJ mol^{-1}) (Fig. 6c). At both growth temperatures, E_{cox} decreased as the leaf O$_2$-consumption rate increased at higher measurement temperatures. As a result, the kinetic model incorporating 'temperature dependence of E_{cox}' also explained the experimental data well, even though the possible values of α were bounded.

Discussion

We constructed a kinetic model in which CP and AP competitively consumed O$_2$, and the model enabled us to analyse the temperature dependence of plant O$_2$-consumption rates and the activation energies of the two pathways. The kinetic model incorporating a temperature dependence of α or E_{cox} satisfactorily reproduced the observed deviations from linearity of the Arrhenius plot of plant O$_2$-consumption rates, as reported in some previous experimental studies. Indeed, in the fitted simulation of the experimental Arabidopsis leaf O$_2$-consumption rates in this study, the fact that the curvature of the Arrhenius plot of plant O$_2$-consumption was fitted well, subject to the condition that α or ΔE changed with the measurement temperature, suggested that rapid changes of α or ΔE, or both, occurred. The fitted simulation suggested that the number of conditions satisfying the observed curvature was higher in the model with variable α than in the model with variable E_{cox}. The pre-exponential factor in the Arrhenius plot has been related to temperature in other models based on transition-state theory or collision theory, whereas we assumed no such relationship for the values of A_{cox} and A_{aox}, the pre-exponential factors related to the CP and AP, respectively, in our kinetic model. Therefore, our kinetic model was more flexible than other models and could include factors other than temperature that might affect the pre-exponential factors in the CP and AP models.

Interpretation of changes of α

Because α in the model is defined as the ratio of [E]$_{0aox}$ to [E]$_{0cox}$, changes in the amount of active AOX protein and electron partitioning through AP (τ_a) should affect the α value. Many previous studies have shown that the amounts of protein in AOX are influenced by environmental factors such as growth temperature (González-Meler *et al.*, 1999; Kurimoto *et al.*, 2004; Fiorani *et al.*, 2005; Watanabe *et al.*, 2008; Umbach *et al.*, 2009), irradiance (Noguchi *et al.*, 2005), plant age (Millar *et al.*, 1998), season (Searle & Turnbull, 2011) and nitrogen availability (Noguchi & Terashima, 2006). Some other studies using the ^{18}O discrimination technique have reported that τ_a is changed by various factors, as follows. During long-term acclimation, τ_a was changed by growth temperature in the leaves of *Populus canadensis* (Searle &
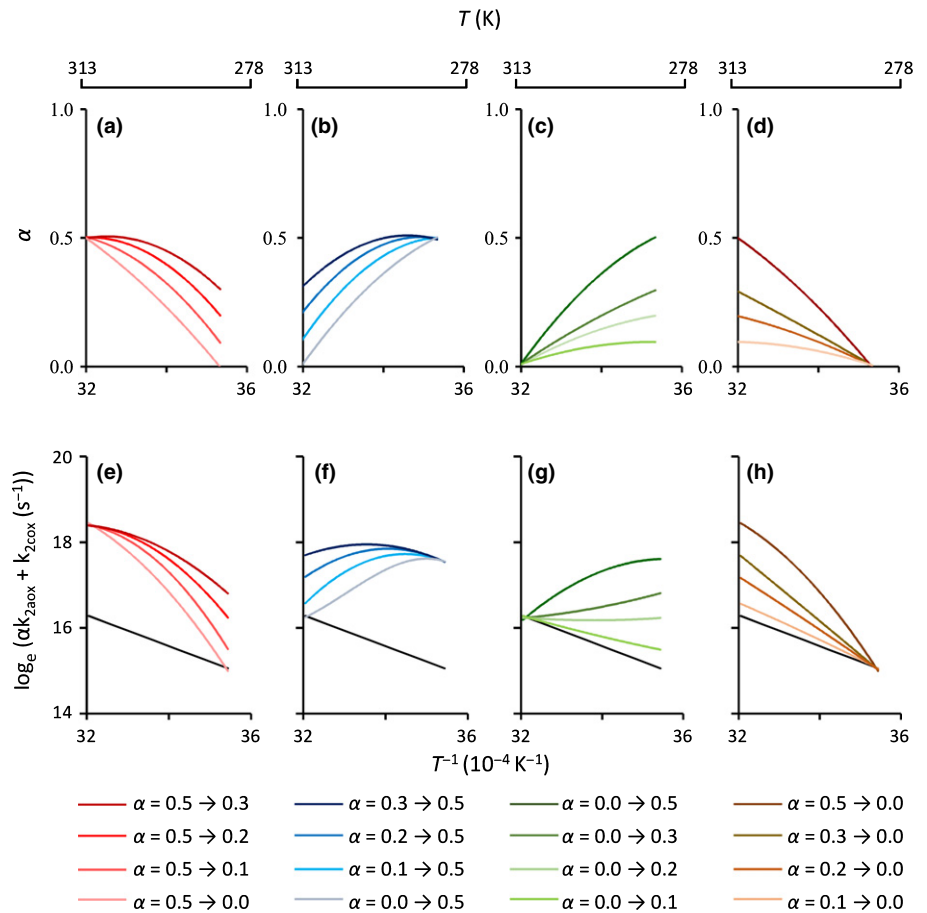
Fig. 4 Profiles of α vs temperature (a–d) that were assumed for the simulations, and the Arrhenius plots produced based on these assumptions (e–h, respectively). In (e–h), the black line indicates the Arrhenius plot when $\alpha = 0$ (no electrons flow to AP). The various convex profiles of α vs temperature were obtained for α in the range 0.0–0.5. A_{cox}, pre-exponential factor related to CP; α, the ratio $[E]_{0aox} : [E]_{0cox}$; $[E]_{0aox}$, the concentration of active AOX in the measurement system; $[E]_{0cox}$, the concentration of active CP in the measurement system; E_{cox}, the activation energy of O_2 reduction by CP; ε, the AP-contribution term in Eqn 13. E_{aox} and E_{cox} were set to 20 kJ mol^{-1} and 30 kJ mol^{-1}, respectively.

Turnbull, 2011) and *Quercus rubra* (Searle *et al.*, 2011a), by the amounts of photosynthetically active radiation in leaves of *Chionochloa rubra* and *Chionochloa pallens* (Searle *et al.*, 2011b), by atmospheric CO_2 concentration in cladodes of *Opuntia ficus-indica* (Gomez-Casanovas *et al.*, 2007), by age in root seedlings of *Glycine max* (Millar *et al.*, 1998) and by the degree of water stress in leaves of *G. max* (Ribas-Carbo *et al.*, 2005). According to our kinetic model, such long-term acclimation is accompanied by changes of α that will be reflected by changes in the magnitude and shape of the Arrhenius plot of plant O_2-consumption rates (Fig. 2).

To our knowledge, only a few studies have described the response of α to rapid temperature changes. Macfarlane *et al.* (2009) monitored electron partitioning through AP (τ_a) and CP (τ_c) in leaf tissues of three plant species (*Cucurbita pepo*, *Nicotiana sativa* and *Vicia faba*) by measuring $^{18}O/^{16}O$ discrimination and O_2-consumption rates at temperatures of 17–36°C. They reported that τ_a values in leaf tissues of the three plant species were invariant with temperature. By contrast, the τ_a in the leaves varied with temperature in the case of Arabidopsis (Armstrong *et al.*, 2008) and *P. canadensis* (Searle & Turnbull, 2011). A slight change of τ_a was also observed in the leaves of *Nicotina tabacum* (Guy & Vanlerberghe, 2005) and in the leaves and hypocotyl of *Vigna radiata* (González-Meler *et al.*, 1999). Still, little is known about the pattern of τ_a response to temperature. Considering that plant mitochondria frequently undergo fusion

and fission within minutes (Arimura *et al.*, 2004; Wakamatsu *et al.*, 2010), rapid changes of α and thus τ_a in response to a temperature change may occur. We can now examine the rapid changes of τ_a in response to temperature by fitting the kinetic model to the curvature of the Arrhenius plot of plant O_2-consumption rates (Fig. 6a,b). The accumulation of data on the instantaneous temperature dependency of τ_a and the fitting of our model to that data may reveal how variations of τ_a affect deviations of Arrhenius plots.

Interpretation of changes of ΔE

Our kinetic model will enable us to examine how the activation energies of the CP and AP respond to temperature changes. Some studies have shown that the instantaneous temperature dependence of O_2-consumption rates differs between CP and AP (McNulty & Cummins, 1987; Collier & Cummins, 1990; Weger & Guy, 1991; Armstrong *et al.*, 2008; Kruse & Adams, 2008; Macfarlane *et al.*, 2009; Kruse *et al.*, 2011). Furthermore, some studies have reported that the instantaneous temperature dependence of the O_2-consumption rates of the two pathways varies when the plants are grown at different temperatures. McNulty & Cummins (1987) reported that Q_{10} – a measure of the instantaneous temperature dependence of leaf O_2-consumption rates – was lower for *Saxifraga cernua* grown at 10°C than at 20°C. The instantaneous temperature dependence of the
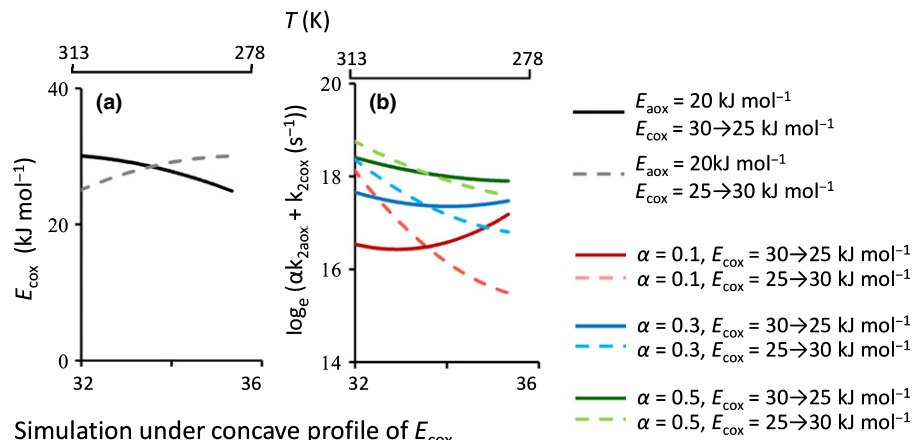
Simulation under convex profile of E_{cox}

Simulation under concave profile of E_{cox}

Fig. 5 Profiles of E_{cox} vs temperature (a, b) that were assumed for the simulations, and the Arrhenius plots generated using these assumptions (c and d, respectively). The values of E_{cox} were in the range 25–30 kJ mol^{-1} in both convex (a) and concave (b) plots. E_{aox} was set to 20 kJ mol^{-1}. A_{cox}, pre-exponential factors related to CP; E_{cox}, the activation energy of the O$_2$ reduction by CP; ε, the AP-contribution term in Eqn 13.

hypocotyl O$_2$-consumption rate was enhanced when *Vigna radiana* was grown at 19°C vs 28°C (González-Meler *et al.*, 1999). Kurimoto *et al.* (2004) have studied several wheat and rice cultivars; they found that the responses of the instantaneous temperature dependence of root O$_2$-consumption rate on growth temperature depended on the cultivar. Furthermore, the instantaneous temperature dependence of the O$_2$-consumption rate (including CP and AP) was influenced by the measurement temperature (Kruse & Adams, 2008; Kruse *et al.*, 2011, 2018). These results suggest that E_{cox}, E_{aox} and ΔE can be changed in response to both long-term and short-term temperature changes. The fact that we also observed differences in the curvatures of Arrhenius plots for Arabidopsis leaf O$_2$-consumption between plants grown at different temperatures suggested that long-term acclimation to growth temperature occurred, and that this long-term acclimation led to differences in the temperature sensitivity to measurement temperature. Our simulation results suggest that electron flow to the AP results in a decrement of the slope of the Arrhenius plot of plant O$_2$-consumption (Figs 2, 3), and a rapid change of ΔE results in curvature of the Arrhenius plot (Figs 5, 6a,c). Further research addressing the underlying mechanisms of long-term and short-term changes in the ambient temperature will be needed.

According to MMRT, the fact that $\Delta C_P^{\ddagger} < 0$ explains the phenomenon that the temperature sensitivity of enzyme-catalysed biochemical reactions decreases with an increase in temperature, and the reaction rate reaches a maximum at a certain temperature T_{opt} (Hobbs *et al.*, 2013; Arcus *et al.*, 2016). In plant O$_2$-consumption, however, concave curvature of an Arrhenius plot – that is, increasing temperature sensitivity of the O$_2$-consumption rate with increasing measurement temperature – has sometimes been observed. Examples include the work of Kruse *et al.* (2018) and the plants grown at 15°C in our study. In our fitting simulation, in which E_{aox}, α, A_{cox}, and A_{aox} were assumed to be independent of the measurement temperature, we were able to fit a concave Arrhenius curve if E_{cox} decreased as the temperature rose (Fig. 6c). This behaviour is consistent with MMRT. The existence of another parallel pathway (e.g. AP) may be an explanation for the concave curvature of Arrhenius plots.

The assumption that $\Delta C_P^{\ddagger} < 0$ in MMRT also explains the negative slope in the Arrhenius plot (i.e. the decrease in the reaction rate with a rise in temperature) at temperatures higher than T_{opt} (Arcus *et al.*, 2016). Umekawa *et al.* (2016) reported a negative activation energy of the O$_2$-consumption rate in the heat-producing flowers of *Symplocarpus renifolius*. They suggested a model in which a negative activation energy could result from biochemical pre-equilibrium reactions comprised of reversible reactions catalysed by cellular dehydrogenases and a rate-determining reaction catalysed by AOX and COX. In their model, the apparent overall activation energy will be negative when the activation energy for the reverse path of the pre-equilibrium reaction
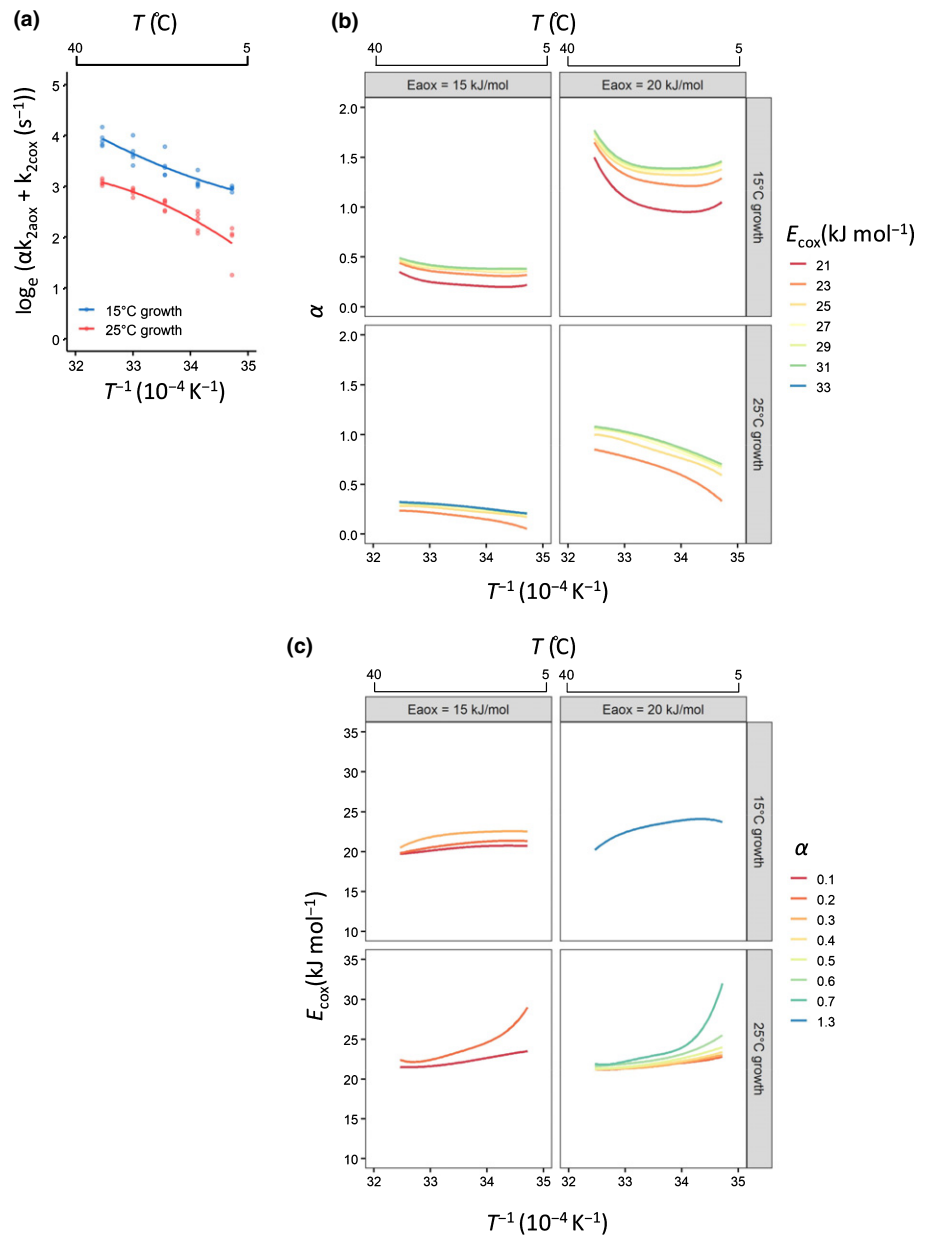
Fig. 6 An Arrhenius plot that deviated from linearity for O_2-consumption rates in leaves of *Arabidopsis thaliana* (Fei-0) (a). Plants were grown for 2 wk at 15°C (blue circles) or 25°C (red circles). The solid lines in (a) indicate the fitted curve of the model described by Eqn 4 ($R^2 = 0.831$ in 15°C grown plants and $R^2 = 0.829$ in 25°C-grown plants). The profiles of α in the fitting simulation assumed that E_{cox} was constant (i.e. independent of measurement temperature) (b), and the profiles of E_{cox} in the fitting simulation assumed that α was constant (i.e. independent of measurement temperature) (c). See the Materials and Methods section for details.

(endothermic reaction) becomes larger than that of the forward reactions (exothermic reactions). Their model is persuasive for understanding plants with heat-producing flowers, and it raises the possibility that the activation energy of some pre-equilibrium reactions may be negative in the respiration of other plants. In addition, our simulation results suggest that negative activation energy may be associated with the reactions of mitochondrial terminal oxidases (AOX and COX) per se.

In some cases, the overall activation energy of CO_2 release by plant leaves is also changed by instantaneous temperature changes (Kruse *et al.*, 2011; Noguchi *et al.*, 2015; Kruse *et al.*, 2018). Furthermore, the fact that the overall activation energy of CO_2 release at the growth temperature, *E (growth)*, shows homeostasis against the growth temperature (Noguchi *et al.*, 2015; Kruse *et al.*, 2018) suggests that the NADH/NAD$^+$ ratio may be

maintained independent of growth temperature in the mitochondrial matrix by adjustment of the rate-determining step of CO_2 release in leaves. Analysis of the instantaneous temperature dependence of plant CO_2 release rates on the basis of a kinetic model may facilitate identification of the rate-determining step of CO_2 release in plants.

Conclusions

We conducted a sensitivity analysis of a theoretical model of plant respiratory O_2-consumption by using the kinetics of CP and AP. Our simulations satisfactorily explained the nonlinearity of Arrhenius plots obtained from experimental rates of plant O_2-consumption. The simulation results indicated the possibility that the AP contribution or activation energy of CP, or both,

New
Phytologist

rapidly changed in response to ambient temperature and that these changes could be the causes of the slope deviations. The fitting simulation suggested that the number of conditions satisfying the observed curvature was higher in the model with variable α than in the model with variable E_{cox}. Simultaneous measurements of the temperature dependence of the O_2-consumption rate and τ_a will reveal in detail the contributions of α and E_{cox}. Furthermore, the effect of the change in the heat capacity, $\Delta C_p^{\ddagger}$, between the reactant and transition state complex in each pathway will be obtained by measuring the O_2-consumption rates of intact tissue or isolated mitochondria (or both) by using inhibitors of CP and AP, respectively. In vivo measurements of electron flows to CP and AP and further analyses of the relationships between activation energies and ambient environmental conditions will help us to understand the plant respiration system.

Author contributions

Both authors discussed and interpreted the data and contributed to drafting and finalising the manuscript.

ORCID

Tomomi Inoue https://orcid.org/0000-0002-2276-4402
Ko Noguchi https://orcid.org/0000-0003-3588-3643

References

Arcus VL, Prentice EJ, Hobbs JK, Mulholland AJ, Van der Kamp MW, Pudney CR, Parker EJ, Schipper LA. 2016. On the temperature dependence of enzyme-catalyzed rates. *Biochemistry* 55: 1681–1688.

Arimura S, Yamamoto J, Aida GP, Nakazono M, Tsutsumi N. 2004. Frequent fusion and fission of plant mitochondria with unequal nucleoid distribution. *Proceedings of the National Academy of Sciences, USA* 101: 7805–7808.

Armstrong AF, Badger MR, Day DA, Barthet MM, Smith PMC, Millar AH, Whelan J, Atkin OK. 2008. Dynamic changes in the mitochondria electron transport chain underpinning cold acclimation of leaf respiration. *Plant, Cell & Environment* 31: 1156–1169.

Atkin OK, Tjoelker MG. 2003. Thermal acclimation and the dynamic response of plant respiration to temperature. *Trends in Plant Science* 8: 343–351.

Collier DE, Cummins WR. 1990. The effects of low growth and measurement temperature on the respiratory properties of five temperate species. *Annals of Botany* 65: 533–538.

Del-Saz NF, Ribas-Carbo M, McDonald AE, Lambers H, Fernie AR, Florez-Sarasa I. 2018. An *in vivo* perspective of the role(s) of the alternative oxidase pathway. *Trends in Plant Science* 23: 206–219.

Dudkina NV, Kouril R, Peters K, Braun H-P, Boekema EJ. 2010. Structure and function of mitochondrial supercomplexes. *Biochemica et Biophysica Acta* 1797: 664–670.

Fiorani F, Umbach AL, Siedow JN. 2005. The alternative oxidase of plant mitochondria is involved in the acclimation of shoot growth at low temperature. A study of Arabidopsis *AOX1a* transgenic plants. *Plant Physiology* 139: 1795–1805.

Gomez-Casanovas N, Blanc-Betes E, Gonzalez-Meler MA, Azcon-Bieto J. 2007. Changes in respiratory mitochondrial machinery and cytochrome and alternative pathway activities in response to energy demand underlie the acclimation of respiration to elevated CO_2 in the invasive *Opuntia ficus-indica*. *Plant Physiology* 145: 49–61.

González-Meler MA, Ribas-Carbo M, Giles L, Siedow JN. 1999. The effect of growth and measurement temperature on the activity of the alternative respiratory pathway. *Plant Physiology* 120: 765–772.

Guy RD, Vanlerberghe GC. 2005. Partitioning of respiratory electrons in the dark in leaves of transgenic tobacco with modified levels of alternative oxidase. *Physiologia Plantarum* 125: 171–180.

Heskel MA, O'Sullivan OS, Reich PB, Tjoelker MG, Weerasinghe LK, Penillard A, Egerton JJG, Creek D, Bloomfield KJ, Xiang J. 2016. Convergence in the temperature response of leaf respiration across biomes and plant functional types. *Proceedings of the National Academy of Sciences, USA* 113: 3832–3837.

Hobbs JK, Jiao W, Easter AD, Parker EJ, Schipper LA, Arcus VL. 2013. Change in heat capacity for enzyme catalysis determines temperature dependence of enzyme catalysed rates. *ACS Chemical Biology* 8: 2388–2393.

Kerbler SM, Taylor NL, Millar AH. 2019. Cold sensitivity of mitochondria ATP synthase restricts oxidative phosphorylation in *Arabidopsis thaliana*. *New Phytologist* 221: 1776–1788.

Kruse J, Adams MA. 2008. Three parameters comprehensively describe the temperature response of respiratory oxygen reduction. *Plant, Cell & Environment* 31: 954–967.

Kruse J, Rennenberg H, Adams MA. 2011. Steps towards a mechanistic understanding of respiratory temperature responses. *New Phytologist* 189: 659–677.

Kruse J, Rennenberg H, Adams MA. 2018. Three physiological parameters capture variation in leaf respiration of *Eucalyptus grandis*, as elicited by short-term changes in ambient temperature, and differing nitrogen supply. *Plant, Cell & Environment* 41: 1369–1382.

Kurimoto K, Millar AH, Lambers H, Day DA, Noguchi K. 2004. Maintenance of growth rate at low temperature in rice and wheat cultivars with a high degree of respiratory homeostasis is associated with a high efficiency of respiratory ATP production. *Plant and Cell Physiology* 45: 1015–1022.

Liang LL, Arcus VL, Heskel MA, O'Sullivan OS, Weerasinghe LK, Creek D, Egerton JJG, Tjoelker MG, Atkin OK, Schipper LA. 2018. Macromolecular rate theory (MMRT) provides a thermodynamics rationale to underpin the convergent temperature response in plant leaf respiration. *Global Change Biology* 24: 1538–1547.

Lloyd J, Taylor JA. 1994. On the temperature dependence of soil respiration. *Functional Ecology* 8: 315–323.

Macfarlane CM, Hansen LD, Florez-Sarasa I, Ribas-Carbo M. 2009. Plant mitochondria electron partitioning is independent of short-term temperature changes. *Plant, Cell & Environment* 32: 585–591.

McNulty AK, Cummins WR. 1987. The relationship between respiration and temperature in leaves of the arctic plant *Saxifraga cernua*. *Plant, Cell & Environment* 10: 319–325.

Milenkovic D, Blaza JN, Larsson N-G, Hirst J. 2017. The enigma of the respiratory chain supercomplex. *Cell Metabolism* 25: 765–776.

Millar AH, Atkin OK, Menz RI, Henry B, Farquhar G, Day DA. 1998. Analysis of respiratory chain regulation in roots of soybean seedlings. *Plant Physiology* 117: 1083–1093.

Millenaar FF, Lambers H. 2003. The alternative oxidase: *in vivo* regulation and function. *Plant Biology* 126: 376–387.

Moore AL, Albury MS, Crichton PG, Affourtit C. 2002. Function of the alternative oxidase: is it still a scavenger? *Trends in Plant Science* 7: 478–481.

Noguchi K, Taylor NL, Millar AH, Lambers H, Day DA. 2005. Response of mitochondria to light intensity in the leaves of sun and shade species. *Plant, Cell & Environment* 28: 760–771.

Noguchi K, Terashima I. 2006. Responses of spinach leaf mitochondria to low N availability. *Plant, Cell & Environment* 29: 710–719.

Noguchi K, Yamori W, Hikosaka K, Terashima I. 2015. Homeostasis of the temperature sensitivity of respiration over a range of growth temperatures indicated by a modified Arrhenius model. *New Phytologist* 207: 34–42.

O'sullivan OS, Weeransinghe KWLK, Evans JR, Egerton JJG, Tjoelker MG, Atkin OK. 2013. High-resolution temperature responses of leaf respiration in snow gum (*Eucalyptus pauciflora*) reveal high-temperature limits to respiratory function. *Plant, Cell & Environment* 36: 1268–1284.

R Core Team. 2019. *R: a language and environment for statistical computing, v.3.6.2.* R Foundation for Statistical Computing, Vienna, Austria. [WWW document] URL https://www.R-project.org/ [Accessed 22 February 2018].

Ribas-Carbo M, Berry JA, Yakir D, Giles L, Robinson SA, Lennon AM, Siedow JN. 1995. Electron partitioning between the cytochrome and alternative pathways in plant mitochondria. *Plant Physiology* 109: 829–837.

Ribas-Carbo M, Taylor NL, Giles L, Busquets S, Finnegan PM, Day DA, Lambers H, Medrano H, Berry JA, Flexas J. 2005. Effects of water stress on respiration in soybean leaves. *Plant Physiology* 139: 466–473.

Schipper LA, Hobbs J, Rutledge S, Arcus VL. 2014. Thermodynamic theory explains the temperature optima of soil microbial processes and high Q10 values at low temperatures. *Global Change Biology* 20: 3578–3586.

Searle SY, Bitterman DS, Thomas S, Griffin KL, Atkin OK, Turnbull MH. 2011a. Respiratory alternative oxidase responds to both low- and high-temperature stress in *Quercus rubra* leaves along an urban-rural gradient in New York. *Functional Ecology* 25: 1007–1017.

Searle SY, Thomas S, Griffin KL, Horton T, Kornfeld A, Yakir D, Hurry V, Turnbull MH. 2011b. Leaf respiration and alternative oxidase in field-grown alpine grasses respond to natural changes in temperature and light. *New Phytologist* 189: 1027–1039.

Searle SY, Turnbull MH. 2011. Seasonal variation of leaf respiration and the alternative pathway in field-grown *Populus × canadensis. Physiologia Plantarum* 141: 332–342.

Seymour RS. 2001. Biophysics and physiology of temperature regulation in thermogenic flowers. *Bioscience Reports* 21: 223–236.

Tjoelker MG, Oleksyn J, Reich PB. 2001. Modelling respiration of vegetation: evidence for a general temperature-dependent Q_{10}. *Global Change Biology* 7: 223–230.

Umbach AL, Lacey EP, Richter SJ. 2009. Temperature-sensitive alternative oxidase protein content and its relationship to flora reflectance in natural *Plantago lanceolata* populations. *New Phytologist* 181: 662–671.

Umekawa Y, Seymour RS, Ito K. 2016. The biochemical basis for thermoregulation in heat-producing flowers. *Scientific Reports* 6: 24830.

Vanlerberghe GC, McIntosh L. 1997. Alternative oxidase: from gene to function. *Annual Review of Plant Physiology and Plant Molecular Biology* 48: 703–734.

Wakamatsu K, Fujimoto M, Nakazono M, Arimura S, Tsutsumi N. 2010. Fusion of mitochondria in tobacco suspension cultured cells is dependent on the cellular ATP level but not on action polymerization. *Plant Cell Reports* 29: 1139–1145.

Watanabe CK, Hachiya T, Terashima I, Noguchi K. 2008. The lack of alternative oxidase at low temperature leads to a disruption of the balance in carbon and nitrogen metabolism, and to an up-regulation of antioxidant defence systems in *Arabidopsis thaliana* leaves. *Plant, Cell & Environment* 31: 1190–1202.

Weger HG, Guy RD. 1991. Cytochrome and alternative pathway respiration in white spruce (*Picea glauca*) roots. Effects of growth and measurement temperature. *Physiologia Plantarum* 83: 675–681.

Supporting Information

Additional Supporting Information may be found online in the Supporting Information section at the end of the article.

Fig. S1 Concave profiles of α vs temperature that were assumed for the simulations, and the Arrhenius plots produced under these assumptions.

Notes S1 Additional details on derivation of equations.

Please note: Wiley Blackwell are not responsible for the content or functionality of any Supporting Information supplied by the authors. Any queries (other than missing material) should be directed to the *New Phytologist* Central Office.